Atmospheric Environment 44 (2010) 2780–2786

Contents lists available at ScienceDirect

Atmospheric Environment

journal homepage: www.elsevier.com/locate/atmosenv

Correlation of methane emissions with cattle population in Argentine Pampas

A. Huarte [a], V. Cifuentes [a,b], R. Gratton [a,c], A. Clausse [a,c,d,*]

[a] Universidad Nacional del Centro, Pinto 399, 7000 Tandil, Argentina
[b] Comisión de Investigaciones Científicas de la Provincia de Buenos Aires, 1900 La Plata, Argentina
[c] Consejo Nacional de Investigaciones Científicas y Técnicas, 1033 Buenos Aires, Argentina
[d] Comisión Nacional de Energía Atómica, 1029 Buenos Aires, Argentina

ARTICLE INFO

Article history:
Received 11 July 2009
Accepted 13 March 2010

Keywords:
Methane inventory
Satellite cartography
Spatial analysis
Top-down methodology
Argentine cattle livestock

ABSTRACT

Satellite cartography of atmospheric methane concentrations during 2003–2004 is applied to a systematic top-down methodology to quantify large scale sources and sinks of this important greenhouse gas. Patterns of methane anomalies over South America below latitude 22 S and an assessment of the emissions from the Buenos Aires Province of Argentina are reported. The latter contains the main cattle livestock of the country together with a variety of surface conditions, both natural and man-modified, influencing methane emissions. It was found that anomalies in methane concentrations may be correlated to emission rates by a simple box accumulation-sweeping model validated by recurrent weather conditions. The model shows that the methane emission rates of the Buenos Aires Province are positively correlated with the cattle livestock corresponding to values of (190 ± 40) g d^{-1} per cattle head.

1. Introduction

The physical transfer of material into a compartment of the world is called emission (Winiwarter and Schimak, 2005). Gas emissions may be estimated from field measurements in combination with statistical data (Billena et al., 2009), which is called the bottom-up approach, used by countries reporting under the United Framework Convention on Climate Change and the Kyoto Protocol. On the other hand, emissions can also be derived from measurement of the concentration distribution and inverse modeling, known as the top-down approach. Inverse is generally carried out from satellite measurements that have the benefit of global coverage (Chance et al., 2000; Abbot et al., 2003; Hoelzemann et al., 2004; Richter et al., 2004; Goede et al., 2007).

In particular, methane emissions are especially relevant for their contributions to climatic change. Men are responsible for about two third of the total methane emission, ~600 Tg year^{-1} (Houweling, 2000, IPCC, 2001). Human-related methane emission (Olivier, 2002) are mainly produced by domestic ruminants, rice fields, carbon mines, waste management, and natural gas usage. In countries where agricultural activities are a major component of economy, like Argentina and New Zealand, the contribution of methane to the total anthropogenic greenhouse gases emissions is comparable to the CO_2 emissions. On the other hand, methane natural sources are mainly constituted by wetlands, including shallow marine water (Heyer and Berger, 2000; Marani and Alvala, 2007). Minor contributions come from termites and non-domestic ruminants (Houweling, 2000). Recent studies suggest that plants emit methane directly as a consequence of metabolic processes (Keppler et al., 2006; Crutzen et al., 2006).

Most of the emitted methane is slowly oxidized in the troposphere through reactions with the OH• radical (Houweling, 2000), although a certain fraction escapes to the stratosphere mainly in the intertropical convergence zone (ITCZ). Furthermore it is transported poleward by the Brewer–Dobson circulation and oxidized through a complex series of reactions, which play an important role in increasing the stratospheric water vapor abundance (Salby, 1996; Bithell et al., 1994). Also, a small fraction of the methane is captured and oxidized in soils (Ridgwell et al., 1999). Although there are some differences between published estimates (Houweling, 2000), the average lifetime of methane in the troposphere of 9 years can be safely assumed, whereas the corresponding lifetime in the stratosphere is much shorter.

Argentine large cattle stock (~50 millions heads) account for 70% of the methane emission of the country due to human activities. Most of the cattle is distributed in the central, east and northeast part of the territory; 22.7 million heads residing in the Buenos Aires Province, whose 310 000 km^2 territory extends between −33° and −41° in latitude and −57° and −63° in longitude. Furthermore, the austral part of Argentina, below latitude −22° includes diverse geographic features potentially associated with methane sources or sinks (*e.g.*, wetlands, lagoons, shallow marine waters, peatlands, continental

* Corresponding author. Universidad Nacional del Centro, Pinto 399, 7000 Tandil, Argentina.
E-mail address: clausse@exa.unicen.edu.ar (A. Clausse).

1352-2310/$ – see front matter © 2010 Elsevier Ltd. All rights reserved.
doi:10.1016/j.atmosenv.2010.03.012

ice-fields). In addition, there are austral forests, rain forests, dry forests, steppes, deserts, extended zones of Holocene volcanism, and large urban centers. Hence, the region constitutes a valuable benchmark case for quantitative evaluation of methane sources and sinks.

Some analyses of methane emissions were recently published for different regions of the world (Keppler et al., 2006; Asadoorian et al., 2006; Zhuang and Reeburgh, 2008; Wratt et al., 2001). The present article presents an analysis of methane satellite data focused in southern South America, particularly the Argentine cattle region. The data set corresponds to good weather conditions and is averaged over a two years period (2003–2004). Using a top-bottom modeling, a cartography of time-averaged emission rates can be produced from the mentioned data.

2. Methane concentration analysis

The satellite data used in the present study were produced by the multichannel infrared spectroscope SCIAMACHY on board of ENVISAT, operating in the nadir mode. The raw data were processed to obtain the methane mixing ratio r average over the atmospheric column in each pixel, which is approximately $0.5^\circ \times 0.5^\circ$ (Frankenberg, 2005; Frankenberg et al., 2005, 2006). Furthermore, r values were averaged and a cloud filtered over the period 2003–2004, *i.e.* values corresponding to measurements taken when the cloud tops exceeded 1 km are discarded. In this way, it can be assured that the data correspond to low cloudiness and vertical stability conditions. Moreover, since the surface albedo is an important restriction to the reliability of r values, the analysis was performed only on data from land masses or shallow waters.

In order to reduce noise, a smoothing procedure was applied by using a three-terms moving average, *i.e.* the value r_{ij} corresponding to the pixel (i, j) is replaced by a smoothed value R_{ij} given by

$$R_{ij} = \frac{r_{i-1,j} + r_{i+1,j} + r_{i,j-1} + r_{i,j+1} + 4r_{i,j}}{8} \quad (1)$$

Fig. 1 shows a map of R in the southern part of South America, limited by the parallel -22° and by the Atlantic and Pacific oceans, from now on called case region. It can be seen that R decreases

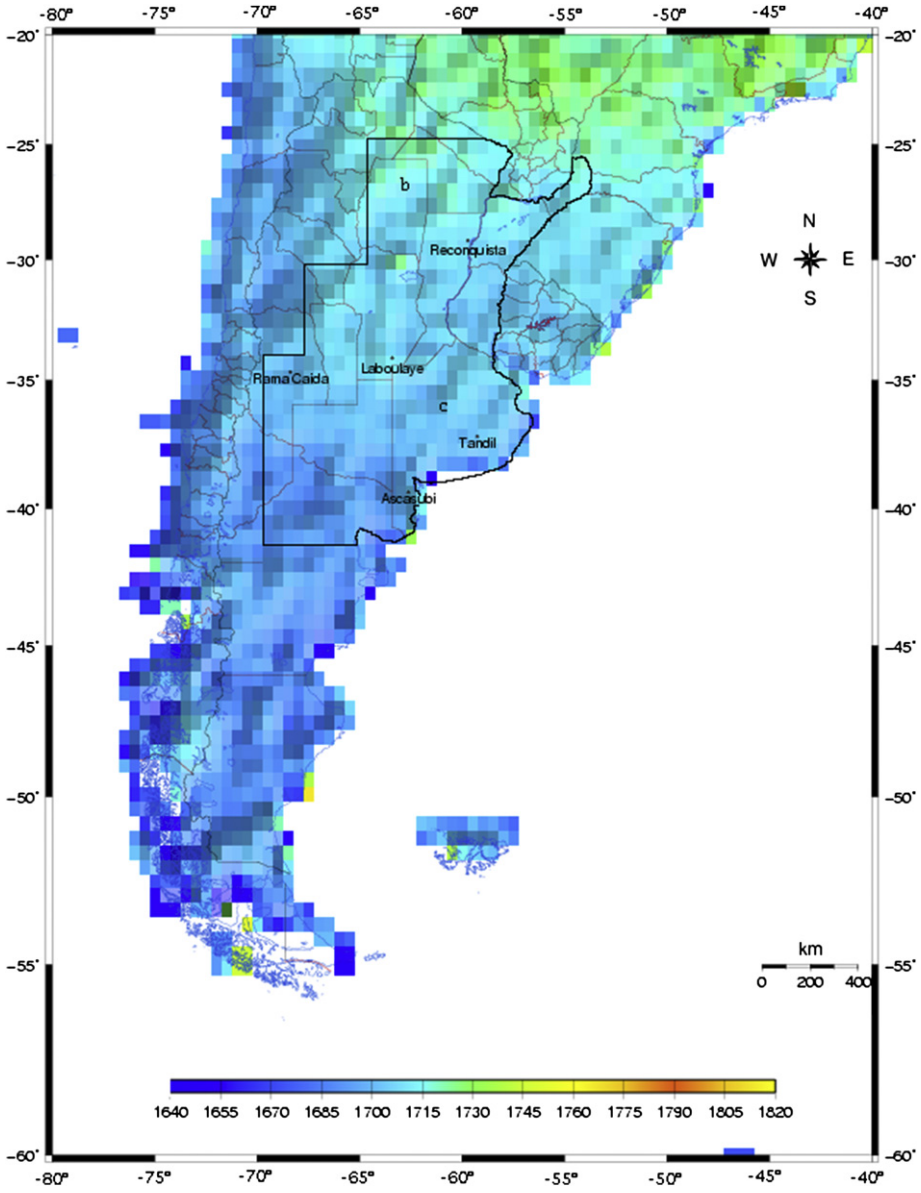

Fig. 1. Methane mixing ratio distribution during 2001–2002 in the southern part of South America.

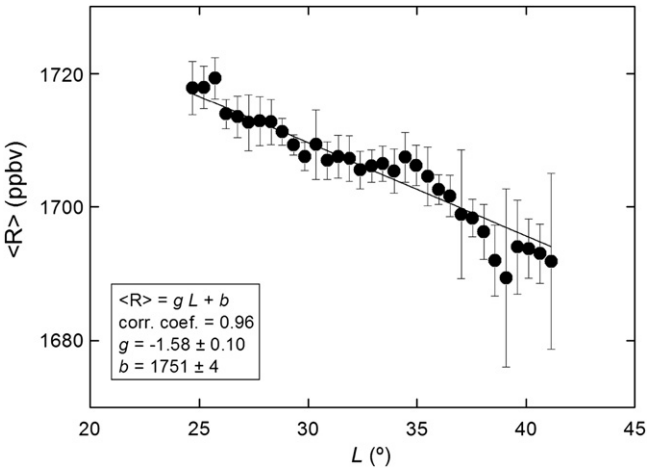

Fig. 2. Latitude dependence of the averaged values of R in subregion b. The bars indicate the standard deviation.

markedly from the tropic poleward. This is a worldwide effect called the South–North (NS) gradient, which is mostly due to the stratospheric methane distribution (Houweling, 2000). In fact, even if only 5–10% of the total methane is above the stratopause, the stratospheric SN gradient at midlatitudes largely exceeds 10 ppbv $^{\circ}L^{-1}$ (Bithell et al., 1994; Salby, 1996).

In order to retrieve a pattern of methane mirroring local surface sources or sinks, the R values should be corrected by subtracting the SN gradient. The magnitude of the latter was calculated selecting a subregion where R is longitudinally uniform, which is labeled b in Fig. 1. This sector excludes Andean region and Patagonia, being mainly a large plain with isolated low mountain ranges. Fig. 2 shows the latitude dependence of R averaged over the longitude in the mentioned subregion b. The error bars indicate the standard deviation. The corresponding linear regression gives a slope $g = -(1.58 \pm 0.10)$ ppbv $^{\circ}L^{-1}$. Subtracting the gradient g, one can define the local methane anomaly as:

$$A_{ij} = (R_{ij} - R_{ref}) - g(L_{ij} - L_{ref}) \quad (2)$$

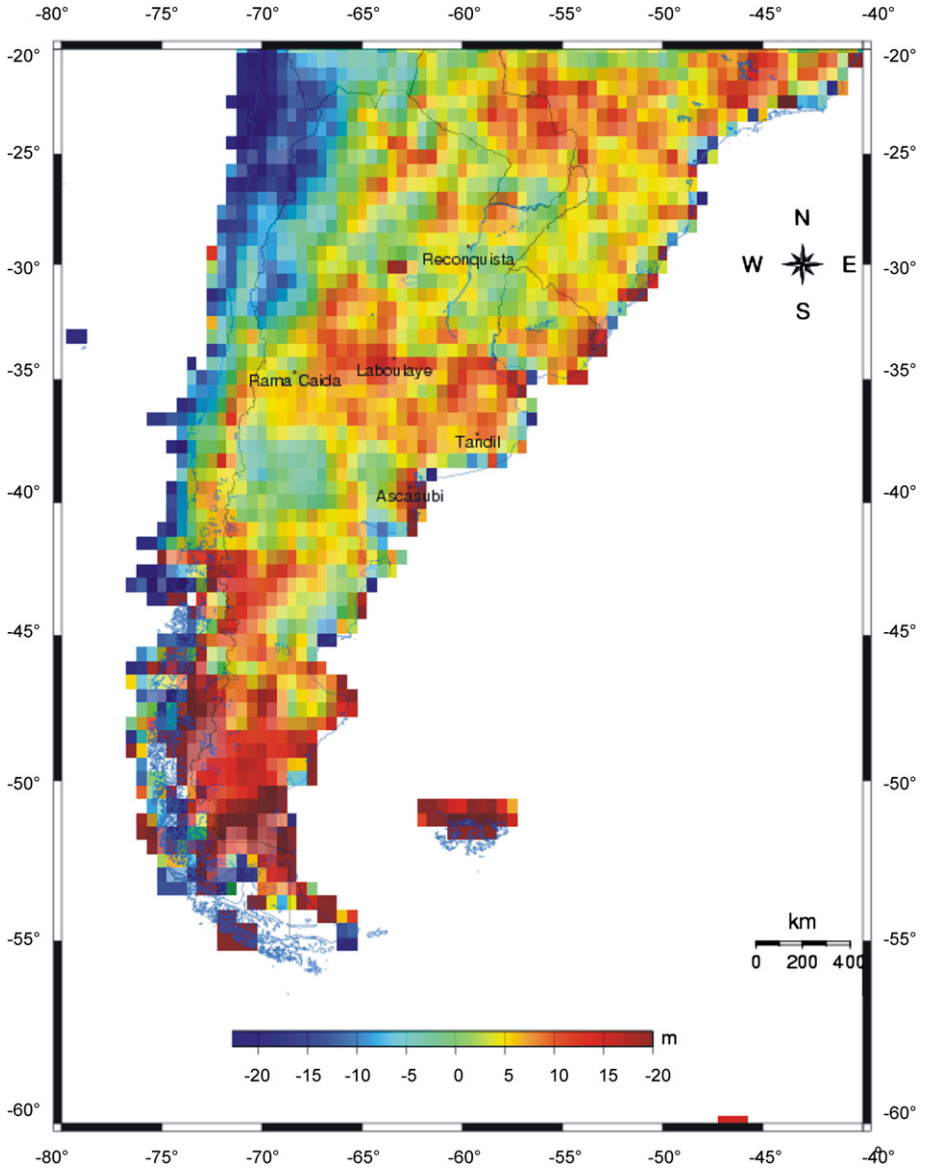

Fig. 3. Methane anomalies in the case region.

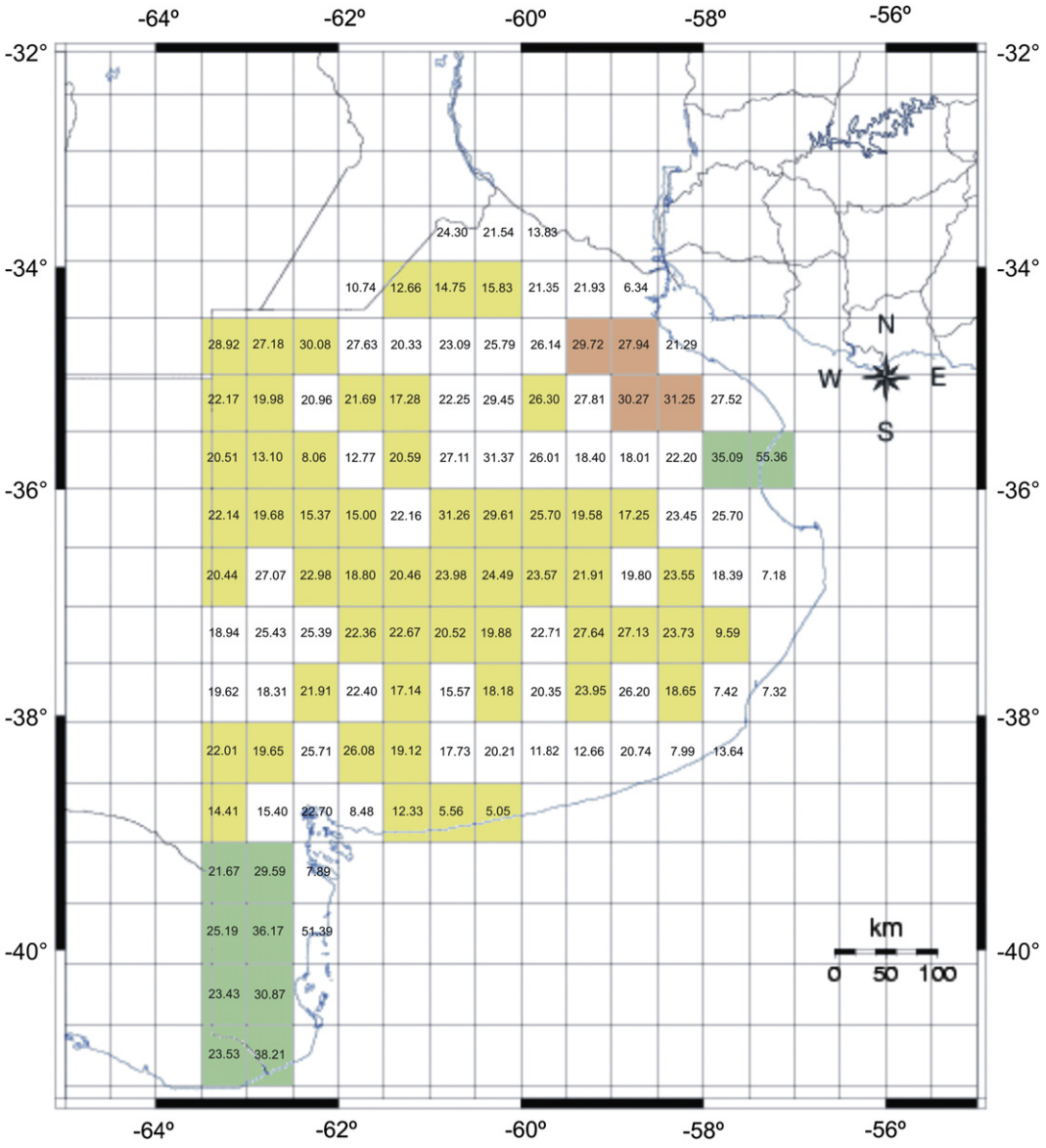

Fig. 4. Methane emission rates in the Buenos Aires Province (mg m^{-2} d^{-1}). The brown pixels are cattle predominant, the green pixels are regions of shallow waters, and the red pixels are metropolitan regions.

where L_{ij} is the local latitude, and $L_{ref}(-38^{\circ})$ and $R_{ref}(1690$ ppbv) are the smoothed methane mixing ratio and the longitude of a reference pixel respectively, which corresponds to a temperate dry steppe almost free from human activities, where the expected methane source is about 0.9 mg m^{-2} d^{-1} (Ridgwell et al., 1999).

Fig. 3 shows the pattern of the methane anomaly in the case region. There is a pronounced negative anomaly associated with the NW sector, mainly a dry plateau located at an altitude ~3300 m, covered in part by large salt flats and characterized by intense Holocene volcanic activity. High uptake rates have been recently found in laboratory measurements of soil samples collected at the periphery of the Campi Flegrei caldera (Castaldi and Tedesco, 2005). The observed uptake was attributed to the abundance of methanotropic batteries selectively favored by the special environmental conditions. That could be also a possible explanation of the observed NW anomaly. In any case, it should be taken into account that high altitude lands increase the relative weight of the stratosphere, which would also explain the anomaly. Also relevant is the positive anomaly in the SW sector, especially below -45°, which extends towards east suggesting a plume-like pattern. This anomaly could be associated with the Patagonic ice-fields (~20 000 km^2) and nearby extended peatlands.

3. Methane emission model

The climate of the subregion *b* is characterized by good weather periods signed by a gradual increase of the daily temperature, which is recurrently interrupted by frontal perturbations with strong winds, vertical instability and sometimes storms or showers, producing sudden temperature drops ~10 °C. The duration τ of each cycle of stable weather was determined by Fourier analyzing the history of the daily temperatures during the period 2001–2006 in a number of agro-meteorological stations distributed in subregion *b*, resulting ~5.5 d.

Based on this recurrent phenomenon, an SBAS model can be produced assuming that during the stable periods between fronts the variation of the methane at each pixel results from the competition between the local emission μ_{ij} and a decay process

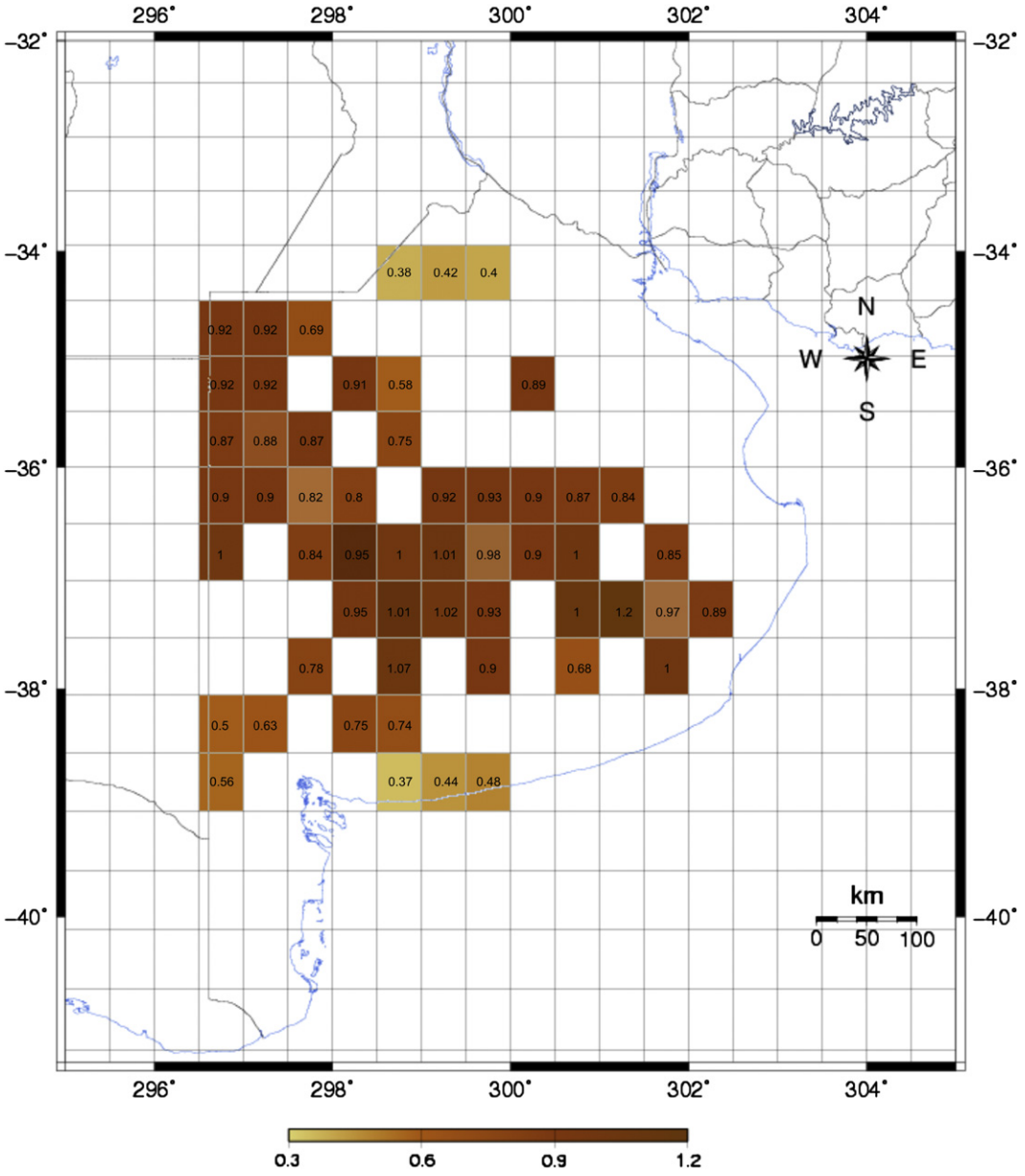

Fig. 5. Average cattle stocking in the Buenos Aires Province (heads per ha).

proportional to the methane concentration. At the end of each period the accumulated methane is then swept-out by the frontal perturbation. Accordingly, between the passages of two successive frontal perturbations A_{ij} (in ppbv units) satisfies:

$$\frac{dA_{ij}}{dt} = \alpha\mu_{ij} - \frac{A_{ij}}{t_o} \tag{3}$$

where t_o is the decay time ($\sim$9 years), and α is a constant coefficient given by 10^9 times the ratio of air and methane molecular weight (1.81) divided by the mass per unit area of the troposphere column overlying the pixel, which is $\sim 8.10^9$ mg m^{-2} at altitudes close to the sea level (*i.e.* $\alpha \cong 0.226$ mg^{-1} m^2).

Solving Eq. (3) leads to:

$$\frac{\langle A_{ij}\rangle}{t_o} = \alpha\mu_{ij} - \alpha\mu_{ij}t_o\left(\frac{1-e^{-\tau/t_o}}{\tau}\right) \tag{4}$$

where $\langle\cdot\rangle$ stands for the time averaging between frontal sweeps. Solving for μ_{ij} yields:

$$\mu_{ij} = \frac{\langle A_{ij}\rangle}{\alpha t_o\left[1 - t_o\left(\frac{1-e^{-\tau/t_o}}{\tau}\right)\right]} \tag{5}$$

Fig. 4 shows the resulting emission rates μ_{ij} in the Province of Buenos Aires. There are two wetlands (green pixels in Fig. 4) located at ($-35.5°$, $-57.5°$) in the shallow south-west sector of River Plata estuary (Samborombon Bay), covering $\sim$3000 km^2, and the marine shallow waters at ($-38.5°$ to $-40.5°$, $-62°$), whose extension is $\sim$10 000 km^2. Pixels at these locations show high μ-values, ranging 30–50 mg m^{-2} s^{-1}. Regarding that these figures are time averages over two years, the values are consistent with direct measurements in midlatitude wetlands, which range from practically null emissions in winter to more than 100 mg m^2 d^{-1} in summer (Zhuang and Reeburgh, 2008). Moreover, all the Buenos Aires Province includes a large number of small scattered lagoons (individual areas ranging from few ha to some km^2) covering an effective area $\sim$15 000 km^2. Assuming that the methane production per unit surface in these scattered

wetlands is similar to the large wetlands (3.85 mg m^{-2} d^{-1}), the total methane production rate due to all the wetlands of the province can be estimated in ~0.64 Tg $year^{-1}$.

There is only one urban area large enough to significantly increase the total emission on the resolution scale: the metropolitan Buenos Aires zone (red pixels in Fig. 4), centered at (−34.7°, −58.5°). The 2000 km^2 urbanized area extended 100 km along the coast and hosts ~12 750 000 inhabitants. The average emission of the urban area results 210 mg m^2 d^{-1}, which is in the range of published values (Lowry et al., 2001). The total urban contribution can be estimated as the average emission of the four pixels corresponding to the metropolitan area times the population ratio between the non-metropolitan and the metropolitan areas. This accounts for an estimated urban contribution of 0.33 mg m^{-2} d^{-1}, and a total urban production rate in the province of ~0.14 Tg $year^{-1}$.

Regarding that the main sources of methane in the region are urban centers, shallow waters and cattle, by subtracting the urban and shallow-waters' contributions from the total emission rate of the province (2.42 Tg $year^{-1}$), the total estimated provincial cattle emission results ~1.64 Tg $year^{-1}$. By dividing the total annual emission attributable to cattle livestock by the 2001–2002 provincial cattle stock (2.27×10^7 heads), we obtain an annual methane emission of 198 g d^{-1} per head. About 90% of the emission per cattle head (*i.e.* ~180 g d^{-1} per head) corresponds to enteric methane, which is in good agreement with field measurements (McGinn et al., 2006; Kebreab et al., 2006). Moreover, the total non-cattle emission rate per unit surface results ~4.18 mg m^{-2} d^{-1}.

The cattle population in each pixel can be calculated from the data produced in the 2001–2002 Argentine National Agriculture Census (INDEC, 2001, 2002). Fig. 5 shows a chart of the number of cattle heads in the significant pixels. The methane emissions, μ, and the cattle density, ρ, of every cattle pixel are plotted in Fig. 6. Although the data are quite dispersed, a certain positive correlation can be appreciated. The Pearson correlation coefficient for the set of data pairs (*i.e.* the covariance of the two variables divided by the product of their standard deviations), which reflects the degree of linear relationship between them, results +0.51. This value suggests that there is linear relation between both variables:

$$\mu = \mu_o + \mu_\rho \rho \tag{6}$$

where μ_ρ is the emission rate per cattle head and μ_o is the emission due to scattered lagoons and towns. Since both variables, ρ and μ, carry uncertainties (σ_μ and σ_ρ), the linear regression should be performed minimizing (Press et al., 2007):

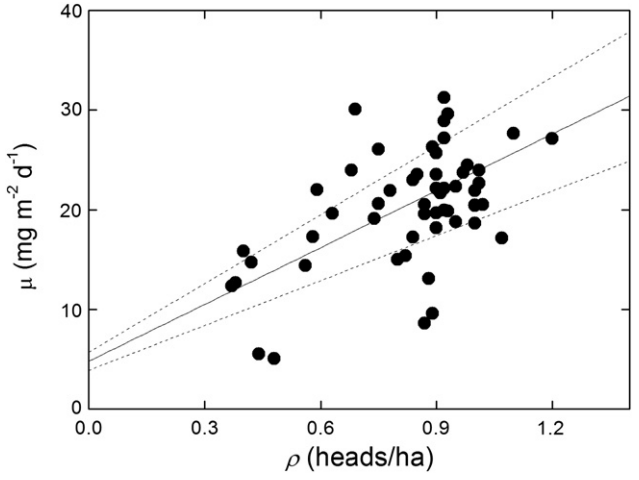

Fig. 6. Correlation between emission and average stock range in the Buenos Aires Province.

$$\chi^2 = \sum_{ij} \frac{(\mu_{ij} - a\rho_{ij} - b)^2}{\sigma_\mu^2 + b^2\sigma_\rho^2} \tag{7}$$

Expressing μ in mg m^{-2} d^{-1} and ρ in cattle heads per ha, results:

$$\mu_\rho = (190 \pm 40) \text{ g } d^{-1} \text{ per head}$$

$$\mu_o = (4.8 \pm 0.9) \text{ mg } m^{-2} \text{ } d^{-1}$$

Both values are consistent with the estimations from the balance of the different methane sources. The error bands showed in Fig. 6 were determined using the constant χ^2 boundaries technique (Press et al., 2007) with 68% of confidence (*i.e.* 68% of the data is contained within constant χ^2 boundaries).

4. Conclusions

By means of the analysis of satellite data, the methane emission rates of the Buenos Aires Province, the main livestock region of Argentina, have been determined with accuracy comparable with the accuracy of bottom-up estimates. It will be very interesting to compare the results reported here for the years 2003–2004 with successive years, looking for spatial variations of the emissions resulting from changes in breeding practices.

Based on the recurrent behavior of the climate conditions of the Pampean region, characterized by good weather periods recurrently interrupted by frontal perturbations, an SBAS model for the dynamics of local methane emissions was proposed, leading to an estimate of the source intensity in each pixel of the analyzed region. The assessment shows an interesting consistency with the cattle population, the shallow waters and urban distributions.

Moreover, the present top-down methodology has proved to be a powerful tool to reveal zones showing unexpected peculiarities worth of specific analysis. In particular the strong anomalies in the NW (negative) and SW (positive) sectors of the southern part of South America are interesting cases for further studies.

Acknowledgements

The authors thank Dr. Chistian Frankenberg for providing the data for this research, and his invaluable comments. This project was supported by ANPCYT, Argentina.

References

Abbot, D., Palmer, P., Martin, R., Chance, K., Jacob, D., Guenther, A., 2003. Seasonal and interannual variability of North American isoprene emissions as determined by formaldehyde column measurements from space. Geophys. Res. Lett. 30 (1886), 4.

Asadoorian, M., Reilly, J., Masurkar, A., 2006. Analyzing Methane-Emitting Activities: Longitudinal Data, Emissions Coefficients, and Spatial Distributions. MIT Joint Program on the Science and Policy of Global Change. Technical Note No. 10.

Billena, N., Roderb, C., Gaiser, T., Stahra, K., 2009. Carbon sequestration in soils of SW-Germany as affected by agricultural management: calibration of the EPIC model for regional simulations. Ecol. Model. 220, 71–80.

Bithell, M., Gray, L., Harries, J., Russell, J., Tuck, A., 1994. Synoptic interpretation of measurements from HALOE. J. Atmos. Sci. 51, 2942–2956.

Castaldi, S., Tedesco, D., 2005. Methane production and consumption in an active volcanic environment of southern Italy. Chemosphere, 131–139.

Chance, K., Palmer, P., Spurr, R., Martin, R., Kurosu, T., Jacob, D., 2000. Satellite observations of formaldehyde over North America from GOME. Geophys. Res. Lett. 27, 3461–3464.

Crutzen, P., Sanhueza, E., Brenninkmeijer, C., 2006. Methane production from mixed tropical savanna and forest vegetation in Venezuela. Atmos. Chem. Phys. Dicuss. 6, 3093–3097.

Frankenberg, C., Meirink, J., van Weele, M., Platt, U., Wagner, T., 2005. Assessing methane emissions from global space-borne observations. Science 308, 1010–1014.

Frankenberg, C., 2005. Retrieval of methane and carbon monoxide using near infrared spectra recorded by SCIAMACHY on board ENVISAT: algorithm development and data analysis. PhD thesis, Ruprecht-Karls-Universität, Heidelberg.

Frankenberg, C., Meirink, J., Bergamaschi, P., Goede, A., Heimann, M., Körner, S., Platt, U., Van Weele, M., Wagner, T., 2006. Satellite cartography of atmospheric methane from SCIAMACHY on board ENVISAT: analysis of the years 2003 and 2004. J. Geophys. Res. 111, D07303.

Goede, A., Burrows, J., Buchwitz, M., 2007. Global mapping of greenhouse gases and air pollutants. Europhys. News 28, 26–32.

Heyer, J., Berger, U., 2000. Methane emission from the coastal area in the southern Baltic Sea. Estuar. Coast. Shelf Sci. 51, 13–30.

Hoelzemann, J., Schultz, M., Brasseur, G., Granier, C., 2004. Global Wildland Fire Emission Model (GWEM): evaluating the use of global area burnt satellite data. J. Geophys. Res. 109, D14S04.

Houweling, S., 2000. Global modeling of atmospheric methane sources and sinks. PhD thesis, Institute for Marine and Atmospheric Research, Utrecht, Utrecht University, The Netherlands, 171 pp.

INDEC, 2001, 2002. Censo Nacional Agropecuario. Resultados Generales. Instituto Nacional de Estadística y Censos. Ministerio de Economía, Buenos Aires, Argentina (in Spanish).

IPCC, 2001. Climate Change 2001: The Scientific Basis, Contribution of Working Group I to the Third Assessment Report of the Intergovernmental Panel on Climate Change. Cambridge University Press, Cambridge, UK.

Kebreab, E., Clark, K., Wagner-Riddle, C., France, J., 2006. Methane and nitrous oxide emissions from Canadian animal agriculture: a review. Can. J. Anim. Sci. 86, 135–158.

Keppler, F., Hamilton, J., Brab, M., Röckmann, T., 2006. Methane emission from terrestrial plants under aerobic conditions. Nature 439, 187–191.

Lowry, D., Holmes, C., Rata, N., 2001. London methane emissions. J. Geophys. Res. 106, 7427–7448.

Marani, L., Alvala, P., 2007. Methane emission from lakes and flood plains in Pantanal, Brazil. Atmos. Environ. 41, 1627–1633.

McGinn, S., Beauchemin, K., Iwaasa, A., McAllister, T., 2006. Assessment of the SF_6 tracer technique for measuring enteric methane emissions from cattle. J Environ. Qual. 35, 1686–1691.

Olivier, J., 2002. On the quality of global emission inventories: approaches, methodologies, input data and uncertainties. PhD thesis, Utrecht University, The Netherlands.

Press, W., Teukolsky, S., Vetterling, W., Flannery, B., 2007. Numerical Recipes: the Art of Scientific Computing, third ed. Cambridge University Press. pp. 773–839.

Richter, A., Eyring, V., Burrows, J., Bovensmann, H., Lauer, A., Sierk, B., Crutzen, P., 2004. Satellite measurements of NO2 from international shipping emissions. Geophys. Res. Lett. 31, L23110.

Ridgwell, A., Marshall, S., Gregson, K., 1999. Consumption of atmospheric methane by soils: a process-based model. Global Biogeochem. Cycles 13, 59–70.

Salby, M., 1996. Fundaments of Atmospheric Physics. Academic Press.

Winiwarter, W., Schimak, G., 2005. Environmental software systems for emission inventories. Environ. Model. Software 20, 1469–1477.

Wratt, D.S., Gimson, N., Brailsford, G., Lassey, K., Bromley, A., Bell, M., 2001. Estimating regional methane emissions from agriculture using aircraft measurements of concentration profiles. Atmos. Environ. 35, 497–508.

Zhuang, Q., Reeburgh, W., 2008. Introduction to special section on synthesis of recent terrestrial methane emission studies. J. Geophys. Res. 113 (G00A02), 3.